

# Electronic structure of alkali-metal/alkaline-earth-metal fluorine beryllium borate $\text{NaSr}_3\text{Be}_3\text{B}_3\text{O}_9\text{F}_4$ single crystal: DFT approach



A.H. Reshak<sup>a,b,\*</sup>, H. Kamarudin<sup>b</sup>, S. Auluck<sup>c</sup>

<sup>a</sup> New Technologies – Research Centre, University of West Bohemia, Univerzitni 8, 306 14 Pilsen, Czech Republic

<sup>b</sup> Center of Excellence Geopolymer and Green Technology, School of Material Engineering, University Malaysia Perlis, 01007 Kangar, Perlis, Malaysia

<sup>c</sup> Council of Scientific and Industrial Research – National Physical Laboratory Dr. K S Krishnan Marg, New Delhi 110012, India

## ARTICLE INFO

### Article history:

Received 29 May 2015

Accepted 6 July 2015

### Keywords:

Optical materials  
Electronic materials  
Inorganic compounds  
Crystal structure  
Semiconductivity  
Wide band gap

## ABSTRACT

The electronic band structure, total and angular momentum resolved projected density of states for  $\text{NaSr}_3\text{Be}_3\text{B}_3\text{O}_9\text{F}_4$  are calculated using the all-electron full potential linearized augmented plane wave plus local orbitals (FP-LAPW + lo) method. The calculations are performed within four exchange correlations namely; local density approximation (LDA), general gradient approximation (PBE-GGA), Engel-Vosko generalized gradient approximation (EVGGA) and the recently modified Becke-Johnson potential (mBJ). Calculations suggest that  $\text{NaSr}_3\text{Be}_3\text{B}_3\text{O}_9\text{F}_4$  is a direct wide band gap semiconductor. The exchange correlations potentials exhibit significant influence on the value of the energy gap being about 4.82 eV (LDA), 5.16 eV (GGA), 6.20 (EVGGA) and 7.20 eV (mBJ). The mBJ approach succeed by large amount in bringing the calculated energy gap closer to the experimental one (7.28 eV). The angular momentum resolved projected density of states shows the existence of a strong hybridization between the various orbitals. In addition we have calculated the electronic charge density distribution in two crystallographic planes namely (101) and (00–1) to visualized the chemical bonding characters.

© 2015 Elsevier B.V. All rights reserved.

## 1. Introduction

Borate crystals are very promising candidates for nonlinear optical (NLO) properties. To obtain second harmonic generation one should have non-centro-symmetric crystals [1–6]. Most borate crystals are used to generate a laser radiation in the infrared and ultraviolet regions. Recently Hongwei Huang et al. [7] synthesized and characterized alkali-metal/alkaline-earth-metal fluorine beryllium borate  $\text{NaSr}_3\text{Be}_3\text{B}_3\text{O}_9\text{F}_4$  in a form of a single crystal. The X-ray diffraction data shows that  $\text{NaSr}_3\text{Be}_3\text{B}_3\text{O}_9\text{F}_4$  crystallizes in the non-centro-symmetric trigonal space group  $R3m$  with  $a = 10.4466(13)$  Å,  $c = 8.3093(17)$  Å, Volume =  $785.3(2)$  Å<sup>3</sup> and  $Z = 3$ . The authors reported that  $\text{NaSr}_3\text{Be}_3\text{B}_3\text{O}_9\text{F}_4$  possesses a very short absorption age, therefore very wide band gap. Hence it is suitable for generating coherent radiation in the deep ultraviolet region. We should emphasize that the incorporation of fluorine in the crystal helps to blue-shift the ultraviolet absorption edge [7]. Chen's group were able to synthesize deep-ultraviolet NLO crystals. They succeeded in growing  $\text{KBe}_2\text{BO}_3\text{F}_2$  (KBBF) which is the first practically usable deep-ultraviolet NLO crystal that can

generate coherent light at the wavelengths 177.3 nm and 193 nm [8–10].

Due to lack of information on the electronic properties of  $\text{NaSr}_3\text{Be}_3\text{B}_3\text{O}_9\text{F}_4$  single crystals, and as natural extension to our previous work on the NLO properties of  $\text{NaSr}_3\text{Be}_3\text{B}_3\text{O}_9\text{F}_4$  single crystals [11] therefore, we thought it is worthwhile to perform comprehensive theoretical calculation based on the density functional theory to investigate the electronic structure and the electron charge density distribution using four exchange correlation potentials in order to ascertain the effect of exchange correlation on the energy band gap and hence to the electronic structure and the related properties. In these calculations we have employed the full potential linear augmented plane wave plus local orbitals (FP-LAPW + lo) method. First-principles calculation is one strong and useful tool to predict the crystal structure and its properties related to the electron configuration of a material before its synthesis [12–15].

## 2. Details of calculation

Using the X-ray diffraction data of Hongwei Huang et al. [7] we have performed a comprehensive theoretical calculation for the electronic band structure, density of states and the electronic charge density distribution for alkali-metal/alkaline-earth-metal

\* Corresponding author at: New Technologies – Research Centre, University of West Bohemia, Univerzitni 8, 306 14 Pilsen, Czech Republic.

E-mail address: [maalidph@yahoo.co.uk](mailto:maalidph@yahoo.co.uk) (A.H. Reshak).

fluorine beryllium borate  $\text{NaSr}_3\text{Be}_3\text{B}_3\text{O}_9\text{F}_4$ . The investigated single crystal belongs to a trigonal space group  $R\bar{3}m$ , the basic building unit of  $\text{NaSr}_3\text{Be}_3\text{B}_3\text{O}_9\text{F}_4$  is the novel anionic group  $[\text{Be}_3\text{B}_3\text{O}_{12}\text{F}]^{10-}$ . The crystal structure is shown in Fig. 1. We employed the full potential linear augmented plane wave plus local orbitals (FP-LAPW + lo) method as implemented in WIEN2k code [16]. This is an implementation of the density functional theory (DFT) with different possible approximations for the exchange–correlation potential. We have used the local density approximation (LDA) [17] and gradient approximation (GGA) [18], which is based on exchange–correlation energy optimization to calculate the total energy. The well-known LDA and GGA underestimation of the band gaps is attributed to the fact that the LDA and GGA Kohn–Sham states do not take into account the quasi-particle self-energy correctly. To overcome this drawback we have used the Engel–Vosko generalized gradient approximation (EVGGA) [19] which is able to reproduce better exchange potential at the expense of less agreement in the exchange energy. This approach yields better band splitting compared to LDA and GGA. Even though EVGGA brings the band gap closer the experimental value it still underestimates the gap by around 1.09 eV. Therefore, we have used the recently proposed modified Becke–Johnson potential (mBJ) [20], which optimizes the corresponding potential for electronic band structure calculations. It is clear that mBJ brings the energy gap to be almost similar to the experimental one. The mBJ a modified Becke–Johnson potential, allows the calculation of band gaps with accuracy similar to the very expensive GW calculations [20]. It is a local approximation to an atomic “exact-exchange” potential and a screening term. We have relaxed the geometry by minimizing the forces acting on each atom. We assume that the structure is totally relaxed when the forces on each atom reach values less than 1 mRy/a.u. To solve the Kohn–Sham equations a basis of linear APW’s were used. In the muffin-tin (MT) spheres the potential and charge density are expanded in spherical harmonics with  $l_{\text{max}} = 8$  and nonspherical components up to  $l_{\text{max}} = 6$ . In the interstitial region the potential

and the charge density are represented by Fourier series. Self-consistency is obtained using 180  $k$  points in the irreducible Brillouin zone (IBZ). The self-consistent calculations are converged since the total energy of the system is stable to within 0.00001 Ry.

### 3. Results and discussion

#### 3.1. Electronic band structure dispersion and density of states

In this section we discuss the electronic band structure, total and the angular momentum resolved projected density of states of  $\text{NaSr}_3\text{Be}_3\text{B}_3\text{O}_9\text{F}_4$  single crystal. The calculated electronic band structures along the high symmetry points are shown in Fig. 2 for all the four exchange correlation potentials. The Fermi level is at 0.0 eV. We find that  $\text{NaSr}_3\text{Be}_3\text{B}_3\text{O}_9\text{F}_4$  possess a wide band gap of 4.82 eV (LDA), 5.16 eV (GGA), 6.20 (EVGGA) and 7.20 eV (mBJ). The conduction band minimum (CBM) and the valence band maximum (VBM) are located at the center of the BZ resulting in a direct band gap. The wide band gap is interesting because it suggests using it for deep ultraviolet nonlinear optical applications. One can see that moving from LDA  $\rightarrow$  GGA  $\rightarrow$  EVGGA  $\rightarrow$  mBJ causes to shift the CBM towards higher energies resulting in opening a bigger gap. It is seen that mBJ brings the energy gap very close to the experimental value of 7.28 eV [7]. The calculated total density of states for LDA, GGA, EVGGA and mBJ are shown in Fig. 3a.

Since mBJ gives the best agreement with the experimental energy gap therefore, we have decided to show the partial density of states for mBJ only in Fig. 3(b–g). The VBM is mainly formed by O1-p, O2-p with small contributions of Sr-p, Be-s/p and O1-s states. The CBM has B-p states as the main contribution whereas Sr-s, Na-s, F1-s, O1-s and O2-s show small contributions. There exists a strong hybridization between various states. In the VB the Na-p state hybridized with Na-s, the Be-s state with B-s, the Be-p state with B-p, the O1-s state with O2-s and finally the O1-s state with O2-p. While in the CB the O1-p state hybridized with O2-p state,

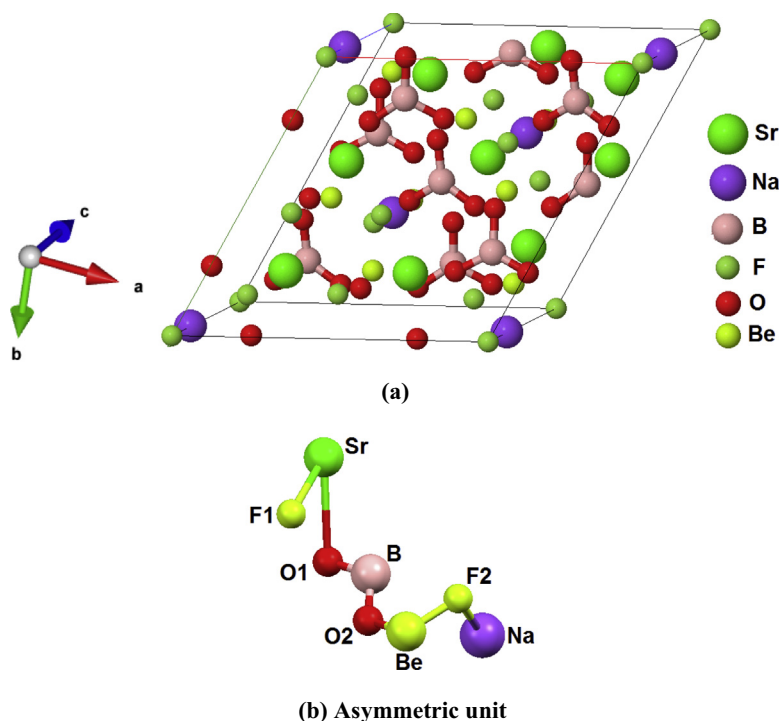
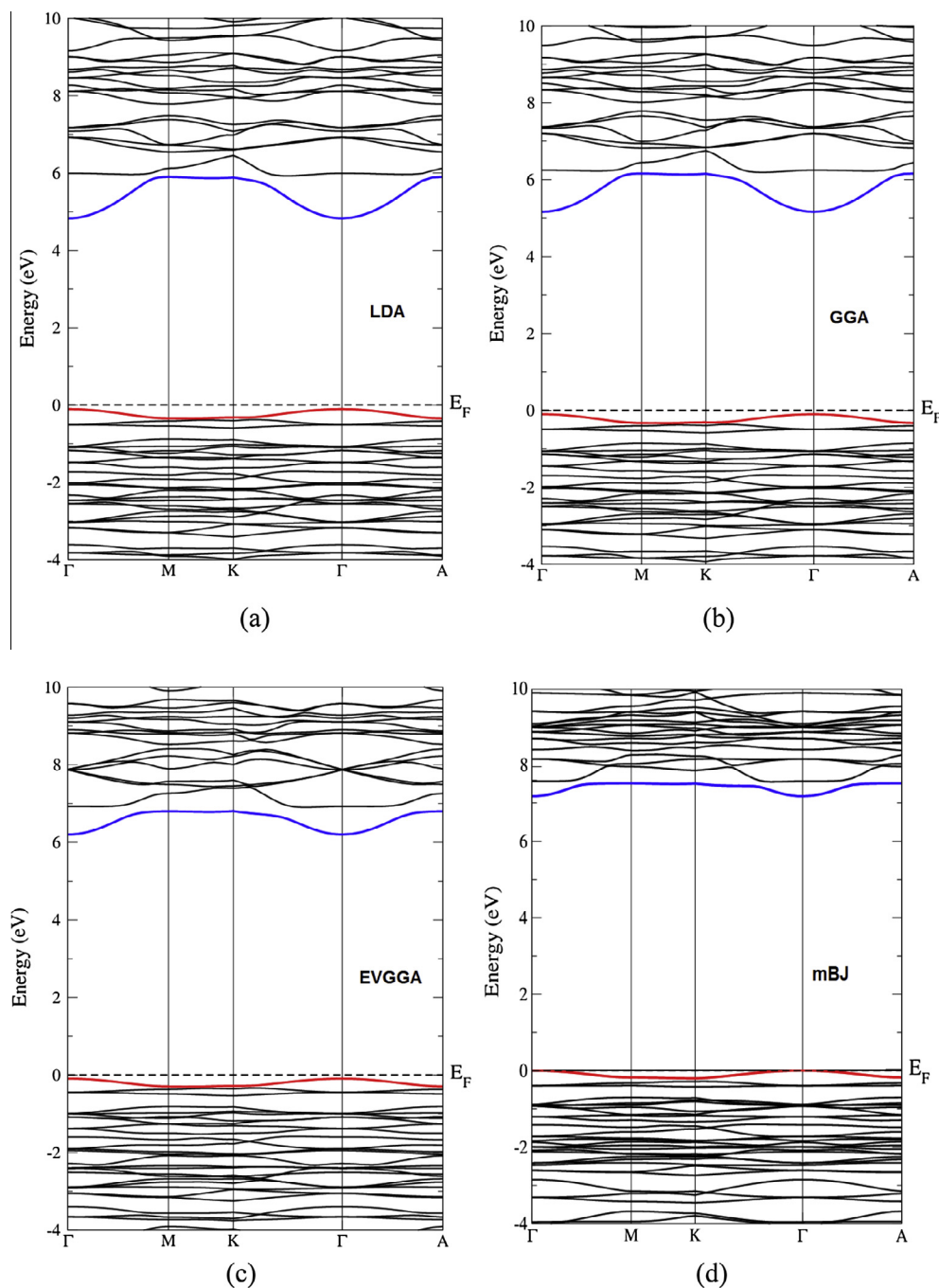


Fig. 1. (a) Fragment of the crystal structure of  $\text{NaSr}_3\text{Be}_3\text{B}_3\text{O}_9\text{F}_4$  single crystal. The B atom is coordinated to three O atoms to form a planar  $\text{BO}_3$  unit. The Be atom is bound to three O atoms and one F atom to form a  $\text{BeO}_3\text{F}$  tetrahedron; (b) asymmetric unit.



**Fig. 2.** The calculated electronic band structure of  $\text{NaSr}_3\text{Be}_3\text{B}_3\text{O}_9\text{F}_4$  single crystal using four exchange correlation potentials; (a) LDA; (b) GGA; (c) EVGGA; (d) mBJ.

the F1-s state hybridized with both of O1-s and O2-s states, the Be-p state hybridized with B-p state, the Na-s state with Na-p, also the Na-p state hybridized with F2-s and finally the Sr-s state hybridized with Sr-p state. The angular momentum resolved projected density of states (PDOS) helps to analyze the nature of the bonds according to a classical chemical concept. This concept is very useful to classify compounds into different categories with respect to different chemical and physical properties. To support this statement we have taken a careful look at the bonding situation since the existence of real hybridization between states of atoms should lead to covalent bond's origin between these atoms. The calculated angular momentum resolved projected density of states below the Fermi level ( $E_F$ ) (PDOS-VB) located between  $-7.0$  eV and  $E_F$  is larger for F1-p (6.0) electron/eV, F2-p (3.0) electron/eV, O1-p

(1.8) electron/eV, O2-p (1.5) electron/eV, B-p (0.45) electron/eV, Be-p (0.14) electron/eV, O1-p (0.17) electron/eV and Sr-p (0.1) electron/eV. Therefore, some electrons from F1, F2, O1, O2, B, Be and Sr atoms are transferred into valence bands and contribute in covalence interactions which is due to the strong hybridization between the states.

The electronic charge density distribution of  $\text{NaSr}_3\text{Be}_3\text{B}_3\text{O}_9\text{F}_4$  was mapped in two crystallographic planes namely (101) and (00–1). These are shown in Fig. 4(a and b). It is seen that (101) plane exhibits Na, Sr, B, F, and O atoms, while (00–1) plane shows only Na and Be atoms. There exists a considerable anisotropy in the physical properties of the investigated material which is important factor for generating the second harmonic (SHG) and optical parametric oscillation (OPO). According to the electro-negativity values

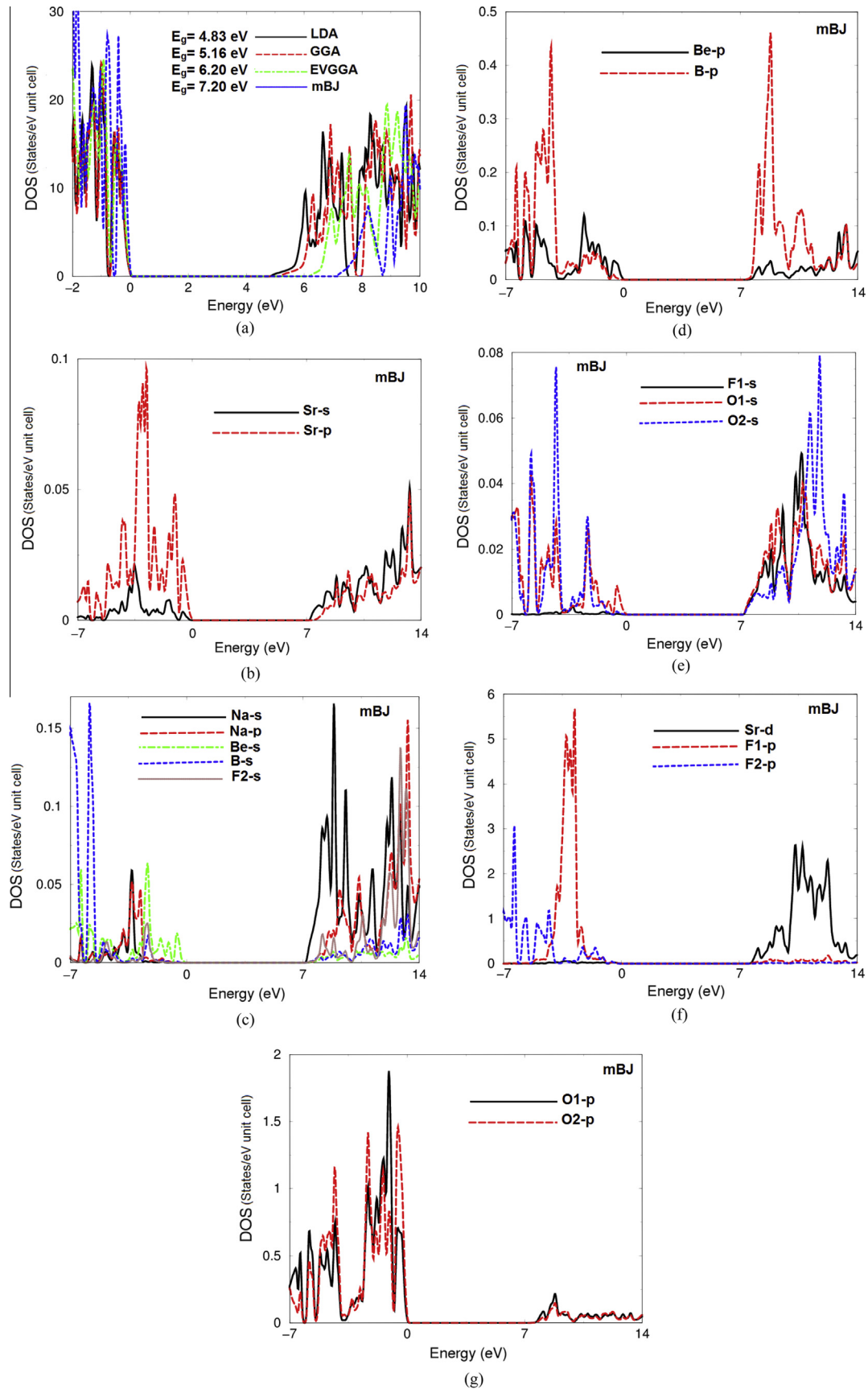


**Fig. 3.** (a) Calculated total density of states (states/eV unit cell) using LDA, GGA, EVGGA and mBJ; (b–g) calculated partial densities of states (states/eV unit cell).

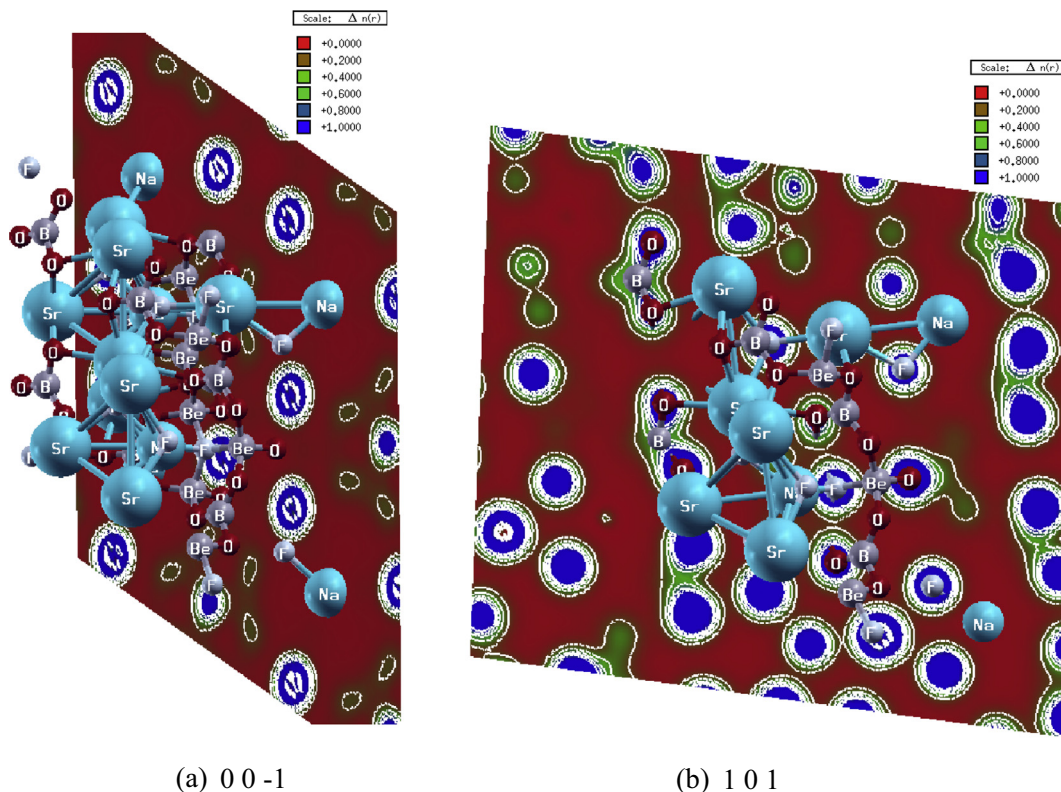


Fig. 4. The electron charge density distribution were calculated for; (a) (101) crystallographic plane; (b) (00–1) crystallographic plane.

Table 1

Calculated bond lengths and angles in comparison to the experimental data [7].

	Exp.	This work
<i>Bond length (Å)</i>		
B–O	1.364(4)–1.398(8)	1.360–1.388
Be–F	1.545(7)	1.539
Be–O	1.561(9)–1.582(5)	1.558–1.579
<i>Bond angles (°)</i>		
O–B–O	117.6(3)–124.8(6)	117.1–124.2

one can see that the charge is attracted towards F atoms (3.98) and O atoms (3.44). This is clearly shown by the blue color surrounding F and O atoms. According to charge density scale the blue color exhibits the highest value (+1.0000) which corresponds to the maximum charge accumulation on the site. The O atoms make strong ionic bonds and partial covalent whereas the F atom forms pure ionic bonds. There is a strong covalent bond between Na (0.93) and Sr (0.95) due to a small electro-negativity difference. The Na forms an ionic bond with F atom, B atoms form partial ionic and partial covalent bonds with O atoms, Sr forms an ionic bond with O atoms, and Be atoms (1.57) form ionic bonds with O and F atoms. The bond lengths and angles were calculated and compared to the experimental data [7], very good agreement was found (see Table 1).

#### 4. Conclusions

Using the X-ray diffraction data of Hongwei Huang et al. we have performed a comprehensive theoretical calculation for the electronic band structure, density of states and the electronic

charge density distribution for alkali-metal/alkaline-earth-metal fluorine beryllium borate  $\text{NaSr}_3\text{Be}_3\text{B}_3\text{O}_9\text{F}_4$  single crystal. We have relaxed the geometry by minimizing the forces acting on each atom. We assume that the structure is totally relaxed when the forces on each atom reach values less than 1 mRy/a.u. The all-electron full potential linearized augmented plane wave plus local orbitals (FP-LAPW + lo) calculations were performed using four exchange correlation potentials. Calculations show that  $\text{NaSr}_3\text{Be}_3\text{B}_3\text{O}_9\text{F}_4$  is a direct wide band gap semiconductor with energy gap of 4.82 eV (LDA), 5.16 eV (GGA), 6.20 eV (EVGGA) and 7.20 eV (mBJ). The mBJ approach brings the calculated energy gap very close to the experimental gap (7.28 eV). The angular momentum resolved projected density of states shows that there exists a strong hybridization between the various orbitals. The electronic charge density distribution was calculated in two crystallographic planes namely (101) and (00–1) which shows that there exists a considerable anisotropy in the physical properties of the investigated material. The bond lengths and angles were calculated and compared to the experimental data, good agreement was found.

#### Acknowledgments

The result was developed within the CENTEM project, reg. no. CZ.1.05/2.1.00/03.0088, cofunded by the ERDF as part of the Ministry of Education, Youth and Sports OP RDI programme and, in the follow-up sustainability stage, supported through CENTEM PLUS (LO1402) by financial means from the Ministry of Education, Youth and Sports under the "National Sustainability Programme I. Computational resources were provided by MetaCentrum (LM2010005) and CERIT-SC (CZ.1.05/3.2.00/08.0144) infrastructures.

S.A. thanks Council of Scientific and Industrial Research (CSIR) – National Physical Laboratory for financial support.

## References

- [1] A.H. Reshak, S. Auluck, I.V. Kityk, Specific features in the band structure and linear and nonlinear optical susceptibilities of La<sub>2</sub>CaB<sub>10</sub>O<sub>19</sub> crystals, *Phys. Rev. B* 75 (2007) 245120.
- [2] A.H. Reshak, Xuean Chen, S. Auluck, I.V. Kityk, X-ray diffraction and optical properties of a noncentrosymmetric borate CaBiGaB<sub>2</sub>O<sub>7</sub>, *J. Chem. Phys.* 129 (2008) 204111.
- [3] A.H. Reshak, S. Auluck, I.V. Kityk, Experimental and theoretical investigations of the first and second order optical susceptibilities of BiB<sub>3</sub>O<sub>6</sub> single crystal, *Appl. Phys. A* 91 (2008) 451–457.
- [4] A.H. Reshak, I.V. Kityk, S. Auluck, Energy band structure and density of states for BaBiBO<sub>4</sub> nonlinear optical crystal, *J. Alloys Compd.* 460 (2008) 99–102.
- [5] A.H. Reshak, S. Auluck, I.V. Kityk, Linear and nonlinear optical susceptibilities for a novel borate oxide BaBiBO<sub>4</sub>: theory and experiment, *J. Solid State Chem.* 181 (2008) 789–795.
- [6] A.H. Reshak, Sushil Auluck, Andrzej Majchrowski, Ivan Kityk, Comparison of the density of states obtained from the X-ray photoelectron spectra with the electronic structure calculations for  $\alpha$ -BiB<sub>3</sub>O<sub>6</sub>, *Japanese J. Appl. Phys.* 48 (2009) 011601.
- [7] Hongwei Huang, Jiyong Yao, Zheshuai Lin, Xiaoyang Wang, Ran He, Wenjiao Yao, Naixia Zhai, Chuangtian Chen, NaSr<sub>3</sub>Be<sub>3</sub>B<sub>3</sub>O<sub>9</sub>F<sub>4</sub>: a promising deep-ultraviolet nonlinear optical material resulting from the cooperative alignment of the [Be<sub>3</sub>O<sub>12</sub>F]<sup>10-</sup> anionic group, *Angew. Chem. Int. Ed.* 50 (2011) 9141–9144.
- [8] C.T. Chen, Z.Y. Xu, D.Q. Deng, J. Zhang, G.K.L. Wong, The vacuum ultraviolet phase-matching characteristics of nonlinear optical KBe<sub>2</sub>BO<sub>3</sub>F<sub>2</sub> crystal, *Appl. Phys. Lett.* 68 (1996) 2930.
- [9] C.T. Chen, N. Ye, J. Lin, J. Jiang, W.R. Zeng, B.C. Wu, Computer-assisted search for nonlinear optical crystals, *Adv. Mater.* 11 (1999) 1071.
- [10] C.T. Chen, G.L. Wang, X.Y. Wang, Z.Y. Xu, Deep-UV nonlinear optical crystal KBe<sub>2</sub>BO<sub>3</sub>F<sub>2</sub>—discovery, growth, optical properties and applications, *Appl. Phys. B* 97 (2009) 9.
- [11] A.H. Reshak, Hongwei Huang, H. Kamarudin, S. Auluck, Alkali-metal/alkaline-earth-metal fluorine beryllium borate NaSr<sub>3</sub>Be<sub>3</sub>B<sub>3</sub>O<sub>9</sub>F<sub>4</sub> with large nonlinear optical properties in the deep-ultraviolet region, *J. Appl. Phys.* 117 (2015) 085703.
- [12] A.H. Reshak, S. Auluck, *Comput. Mater. Sci.* 96 (2015) 90–95.
- [13] Hardev S. Saini, Mukhtiyar Singh, A.H. Reshak, Manish K. Kashyap, *Comput. Mater. Sci.* 74 (2013) 114–118.
- [14] A.H. Reshak, T. Ouahrani, R. Khenata, A. Otero-de-la-Roza, V. Luana f, H. Baltache, *Comput. Mater. Sci.* 50 (2011) 886–892.
- [15] Shiwu. Gao, Linear-scaling parallelization of the WIEN package with MPI, *Comput. Phys. Commun.* 153 (2003) 190.
- [16] P. Blaha, K. Schwarz, G.K.H. Madsen, D. Kvasnicka, J. Luitz, WIEN2k, An augmented plane wave plus local orbitals program for calculating crystal properties, Vienna University of Technology, Austria, 2001.
- [17] W. Kohn, L.J. Sham, Self-consistent equations including exchange and correlation effects, *Phys. Rev. A* 140 (1965) 1133.
- [18] J.P. Perdew, S. Burke, M. Ernzerhof, Generalized gradient approximation made simple, *Phys. Rev. Lett.* 77 (1996) 3865.
- [19] E. Engel, S.H. Vosko, Exact exchange-only potentials and the virial relation as microscopic criteria for generalized gradient approximations, *Phys. Rev. B* 47 (1993) 13164.
- [20] Fabien Tran, Peter Blaha, Accurate band gaps of semiconductors and insulators with a semilocal exchange–correlation potential, *Phys. Rev. Lett.* 102 (2009) 226401.